Separation Science and Technology
Publication details, including instructions for authors and subscription information:
http://www.informaworld.com/smpp/title~content=t713708471

Removal of Phenol by Adsorption on Powdered Activated Carbon in a Continuous Flow Stirred Cell Membrane System

H. W. Lee[a]; K. J. Kim[b]; A. G. Fane[b]
[a] DEPARTMENT OF CHEMICAL ENGINEERING, CHEJU NATIONAL UNIVERSITY, CHEJU, KOREA
[b] UNESCO CENTRE FOR MEMBRANE SCIENCE AND TECHNOLOGY SCHOOL OF CHEMICAL ENGINEERING AND INDUSTRIAL CHEMISTRY, UNIVERSITY OF NEW SOUTH WALES, SYDNEY, AUSTRALIA

To cite this Article Lee, H. W. , Kim, K. J. and Fane, A. G.(1997) 'Removal of Phenol by Adsorption on Powdered Activated Carbon in a Continuous Flow Stirred Cell Membrane System', Separation Science and Technology, 32: 11, 1835 — 1849
To link to this Article: DOI: 10.1080/01496399708000740
URL: http://dx.doi.org/10.1080/01496399708000740

SEPARATION SCIENCE AND TECHNOLOGY, **32**(11), pp. 1835–1849, 1997

Removal of Phenol by Adsorption on Powdered Activated Carbon in a Continuous Flow Stirred Cell Membrane System

H. W. LEE
DEPARTMENT OF CHEMICAL ENGINEERING
CHEJU NATIONAL UNIVERSITY
CHEJU 690-756, KOREA

K. J. KIM* and A. G. FANE
UNESCO CENTRE FOR MEMBRANE SCIENCE AND TECHNOLOGY
SCHOOL OF CHEMICAL ENGINEERING AND INDUSTRIAL CHEMISTRY
UNIVERSITY OF NEW SOUTH WALES
SYDNEY 2052, AUSTRALIA

ABSTRACT

This work presents a fundamental study for prediction of breakthroughs in a continuous flow membrane system containing powdered activated carbon (PAC) for phenol removal. The adsorption isotherm of phenol on PAC typically followed the Freundlich equation. A surface diffusion model was employed to simulate the adsorption of phenol in the systems. The model agrees well with the experimental breakthrough data, and it could be effectively applied to predict the breakthrough curve for design of adsorption-membrane filtration system. Intraparticle transport appears to be the rate-limiting step in this system. Surface diffusivity (D_s) obtained by fitting the model breakthrough curve to that of the experiment was 3.3×10^{-8} $cm^2 \cdot s^{-1}$.

Key Words. Mathematical model; Microfiltration membrane; Phenol removal; Powdered activated carbon; Breakthrough curves

---

* To whom correspondence should be addressed.

INTRODUCTION

A number of researchers (1–6) have shown that membrane technology can provide interesting alternatives to conventional methods for removal and recovery of phenol from waste streams. However, the removal of low molecular weight species such as dissolved organic matter is limited due to its tendency to low rejection and membrane fouling. Accordingly, there is a growing interest in coupling membranes with other unit processes to give a hybrid process with better performance than either of the component parts. For removal of dissolved organics, membrane hybrid systems with adsorbent or ion exchanger have been attempted (7–10). A packed-bed or continuous flow stirred tank can be used for separation of organics with adsorbents. Most studies of adsorption with activated carbon have used packed beds (11, 12), and little work has been done with the continuous flow stirred tank.

The mass transfer associated with the adsorption of solutes from solution by porous adsorbents occurs via the three consecutive steps of bulk, film, and intraparticle transport (12). Intraparticle transport involves two mass transfer processes, pore and surface diffusion, which act in parallel. The pore diffusion considers the solute diffusing within intraparticle pore voids and adsorbing on vacant pore wall sites in a localized and laterally immobile manner. The surface diffusion mechanism assumes adsorption on the solid surface and then migration of adsorbate along the interface. Although intraparticle mass transfer dynamics can be described by both pore and surface diffusion, a number of investigators (12–14) have shown that surface flux generally predominates and that pore flux can be neglected. In other words, intraparticle mass transfer can be described by a surface diffusion model only.

This study investigates the removal of phenol by PAC adsorption and membrane filtration. Experiments were performed to obtain the breakthrough data for different operating conditions. The parameters studied include suspended PAC inventory, cell holdup volume, stirring speed, feed flow rate, and feed concentration. A mathematical model was developed for a continuous adsorption–filtration system. The predicted breakthrough curves generated from the model were compared with the experimental results.

MATHEMATICAL MODEL

This model assumes the following:

1. Spherical activated carbon of uniform size
2. Film type resistance in external mass transfer

3. Surface diffusion as the predominant intraparticle mass transfer
4. Surface diffusivity is concentration independent
5. Local equilibrium adjacent to the activated carbon surface

The transient response of the system can be obtained from the following set of equations. Mobile phase mass balance:

$$\epsilon V\frac{\partial C}{\partial t} = UF - UC - \rho_p V_{\mathrm{holdup}}(1 - \epsilon)\left(\frac{3}{R}\right)\frac{\partial q}{\partial r}\bigg|_{t=R} \tag{1}$$

Intraparticle diffusion:

$$\frac{\partial q}{\partial t} = D_s\left(\frac{2\partial q}{\mathrm{r}\,\partial r} + \frac{\partial^2 q}{\partial r^2}\right) \tag{2}$$

Adsorption isotherm:

$$C_e = f(q_e) \tag{3}$$

Initial conditions:

$$C = 0, \qquad \text{at } t = 0 \tag{4}$$

$$q = 0, \qquad \text{at } t = 0, 0 \leq r \leq R \tag{5}$$

Boundary conditions:

$$\frac{\partial q}{\partial r} = 0, \qquad \text{at } r = 0 \tag{6}$$

$$k_f\,(C - C_s) = \rho_p D_s\frac{\partial q}{\partial r}\bigg|_{r=R} \tag{7}$$

To obtain transient response, the simultaneous partial differential Eqs. (1)–(3) were solved by the finite differential method. Surface diffusivity (D_s) was determined by fitting the model breakthrough curve to that of the experiment, in which the golden section method (15) was employed for the one-dimensional parameter estimation. All the computations were done using a VAX.

EXPERIMENTAL

Apparatus

The schematic experimental set up is shown in Fig. 1. All experiments were performed in a cell of 110 mL capacity and with a membrane area of 15.2 cm^2. The cell consists of a cylindrical vessel containing the test solution, surmounting a porous support on which the membrane is placed. Details of the cell are given elsewhere (16).

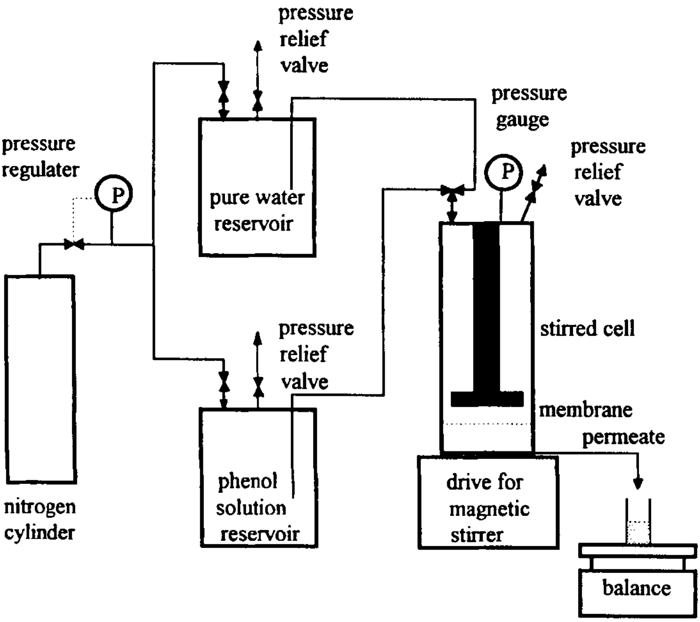

FIG. 1 Schematic diagram of experimental apparatus.

Membrane

The membrane used was Millipore VVLP microfilter (pore diameter 0.1 μm, hydrophilic) and its resistance, R_m, calculated from the pure water flux averaged 5.6×10^{10} cm^{-1}.

Chemicals

Phenol was of analytical grade obtained from Ajax Chemicals. Distilled water was obtained from a Milli Q system with a conductivity of <0.05 μS.

Untreated activated charcoal (100–400 mesh; Sigma product C 5260), purchased from Sigma Chemicals (USA), was sieved with a 75–125 μm mesh siever and washed several times with distilled water for removal of undersized particles. The particles was then oven dried at 110°C for 2 days and stored in a desiccator. The surface area for this product is 750 $m^2 \cdot g^{-1}$ according to the manufacturer. The particle size distributions obtained using a Malvern Mastersizer (Malvern Co., UK) are presented in Fig. 2, with a mean particle size of 114.6 μm. The true density was 2.29

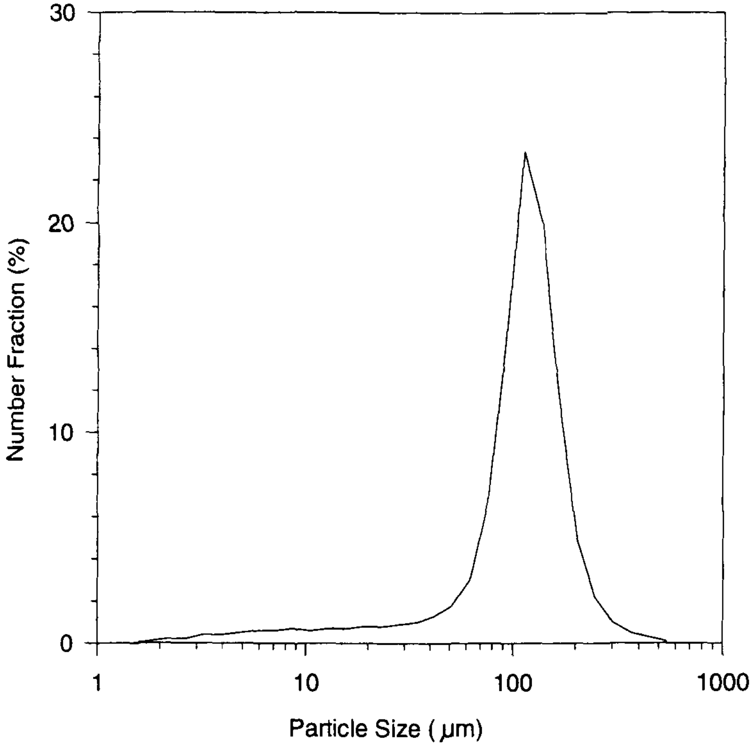

FIG. 2 Particle size distribution of activated carbon.

$g \cdot cm^{-3}$ determined using an Autopycnometer (Micrometrics Helium Air Pycnometer 1320).

Equilibrium Studies

The adsorption isotherm for phenol on PAC was obtained by adding a given amount of PAC to a flask containing a given amount of phenol solution and agitating at 22 ± 1°C until the equilibrium state was reached. Equilibrium was achieved within about a week. After equilibrium, all samples were filtered through a 0.2-μm membrane prior to analysis to eliminate interferences from the carbon fines in the supernatant. The resultant phenol concentration was determined by a Varian 1E Spectrophotometer (Varian Australia P/L) at a wavelength of 268 nm. The amount of the phenol adsorbed on the PAC, q, was obtained by mass balance, i.e., $q = [(C_i - C_e)V]/W$.

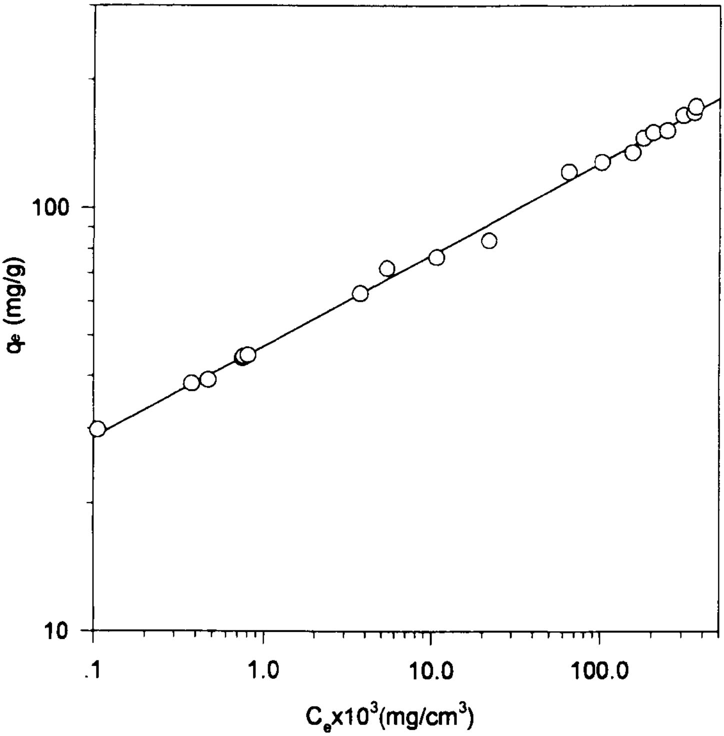

FIG. 3 Adsorption isotherm for PAC–phenol system.

The experimental data followed a typical Freundlich isotherm (17), as shown in Fig. 3.

$$q_e = K_F C_e^{1/n} = 213.4 C_e^{0.219}$$

Filtration Procedure

A given amount of activated carbon was added to the cell containing a given amount of distilled water, and filtration was carried out with replenishment of distilled water for about an hour until the flux was at steady state. When steady state was reached the distilled water was replaced by phenol solution (concentration in the 100 to 400 ppm range), which was continuously fed from a feed reservoir connected to the cell. Operating conditions were maintained at 22 ± 1°C, with transmembrane pressures in the 10 to 56 kPa range and with stirring speeds of 300, 600, and 900 rpm. The instantaneous flux was measured gravimetrically by an electronic balance.

RESULTS AND DISCUSSION

The results are presented as plots of normalized permeate concentration (ratio of permeate to feed concentration) as a function of time.

Effect of PAC Amount in Suspension

Figure 4 shows experimental and predicted breakthrough curves for different amounts of activated carbon. The predicted profiles are expressed as lines according to the model. The film mass transfer k_f in Eq. (7) was calculated from Eq. (8) by Ranz and Marshall (18).

$$\mathrm{Sh_p} = \frac{d_p k_f}{D_m} = 2 + 0.60\mathrm{Re_p^{1/2}Sc^{1/3}} \tag{8}$$

$\mathrm{Re_p}$, which is a function of particle-fluid relative velocity, can be calcu-

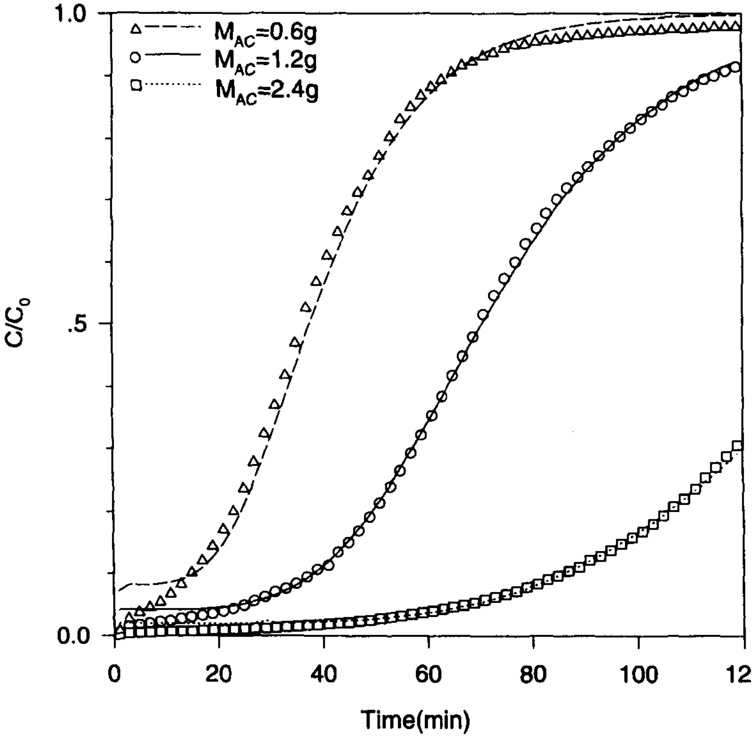

FIG. 4 Breakthrough curves for different amounts of activated carbon. The symbols represent experimental data and the lines represent predicted profiles. $C_0 = 0.2$ mg/cm^3, $V' = 0.19$ cm^3/s, $V_{\mathrm{holdup}} = 70$ cm^3, $N = 600$ rpm.

lated from Kolmogoroff's theory (19, 20). According to the theory, eddy size, η, can be expressed by Eq. (9) and then related to Re_p by Eqs. (10) and (11), depending on particle size.

$$\eta = \left(\frac{\nu^3}{E_D}\right)^{1/4} \tag{9}$$

For particles $\eta \ll d_p$,

$$Re_p = \left(\frac{E_D d_p^4}{\nu^3}\right)^{1/3} \tag{10}$$

For particles $\eta \gg d_p$,

$$Re_p = \left(\frac{E_D d_p^4}{\nu^3}\right)^{1/2} \tag{11}$$

Here the energy dissipation rate, E_D can be obtained from Eq. (12), for which $N_p = 1.2$ was used for the system in this study (21, 22).

$$E_D = \frac{P}{W} = \frac{N_p \rho_L N^3 d_I^5}{W} \tag{12}$$

When $V = 70\ \mathrm{cm}^3$ and $N = 600$ rpm, the k_f value calculated was $1.64 \times 10^{-2}\ \mathrm{cm \cdot s^{-1}}$, where $D_m = 1.11 \times 10^{-5}\ \mathrm{cm^2 \cdot s^{-1}}$ was obtained from Wilke and Chang (23). The determined surface diffusivity was $3.3 \times 10^{-8}\ \mathrm{cm^2 \cdot s^{-1}}$ and agreed well with experimental results. The determined value of surface diffusivity ($3.3 \times 10^{-8}\ \mathrm{cm^2 \cdot s^{-1}}$) compares reasonably well with other values reported in the literature (24–26) for phenol sorption on activated carbon. Streat et al. (24) reported values in the 1.41 to $3.8 \times 10^{-8}\ \mathrm{cm^2 \cdot s^{-1}}$ range at 21°C for most activated carbons derived from coal and wood, but a somewhat lower values for coconut shell carbon. Using Calgon Filtersorb 400 granular activated carbon (Calgon Corp) and phenol, Crittenden and Weber (25) and Sorial et al. (26) reported surface diffusivity values of 3.53×10^{-8} and $8.629 \times 10^{-8}\ \mathrm{cm^2 \cdot s^{-1}}$, respectively.

The initially lower experimental results relative to the predicted data could be due to accumulation of PAC at the membrane surface.

Effect of Holdup Volume

Breakthrough profiles for varying holdup volumes in cells of 40, 70, and 100 cm^3, given in Fig. 5, show that there was only a minor effect of

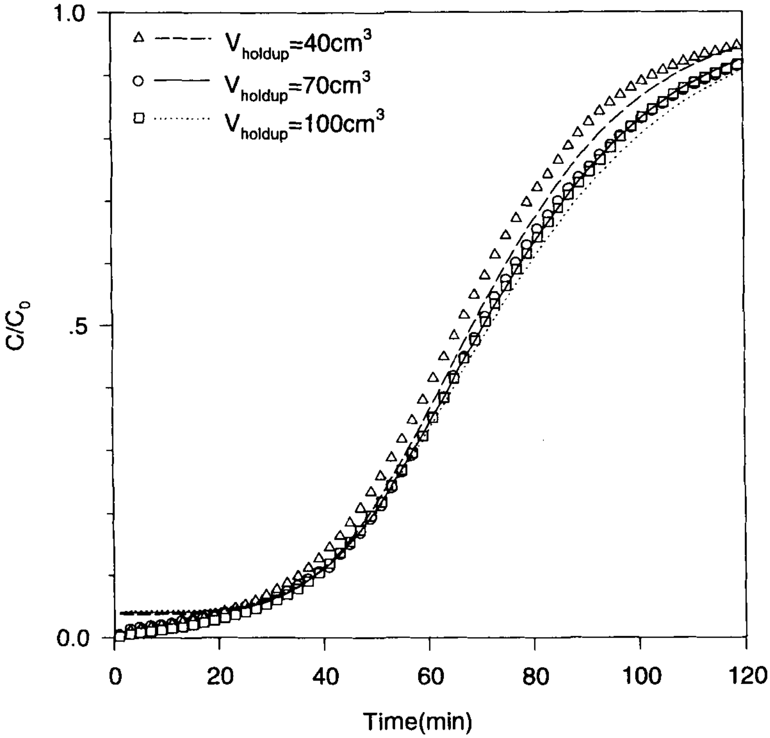

FIG. 5 Breakthrough curves for different hold-up volumes. The symbols represent experimental data and the lines represent predicted profiles. C_0 = 0.2 mg/cm^3, V' = 0.19 cm^3/s, M_{AC} = 1.2 g, N = 600 rpm.

holdup volume in the cell on the breakthrough behavior. However, the smallest holdup volume shows a faster approach to adsorption capacity of PAC (i.e., normalized concentration = 1). This is similar to the behavior of an ideal continuous stirred tank reactor where no adsorption is occurring. Experimental and simulation results using the same value for the diffusivity obtained in the previous section were in good agreement.

In the case of different holdup volumes, the breakthrough behavior would be influenced only by the film mass transfer coefficient. For holdup volumes of 40, 70, and 100 cm^3 the film mass transfer coefficients calculated from Eqs. (8)–(12) were 1.79×10^{-2}, 1.64×10^{-2}, and 1.56×10^{-2} cm·s^{-1}, respectively.

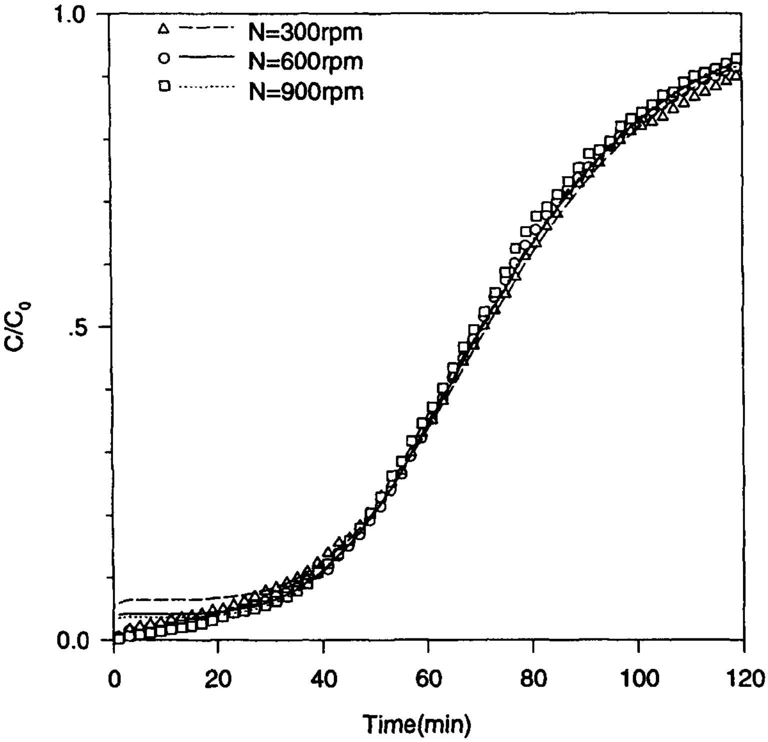

FIG. 6 Breakthrough curves for varying stirring speeds. The symbols represent experimental data and the lines represent predicted profiles. C_0 = 0.2 mg/cm^3, V' = 0.19 cm^3/s, M_{AC} = 1.2 g, V_{holdup} = 70 cm^3.

Effect of Stirring Speed

Figure 6 shows the breakthrough profiles for stirring speeds of 300, 600, and 900 rpm for both experimental and calculated data. A minor effect of stirring was found for the breakthrough behavior, implying that the rate-limiting step in this system is intraparticle transport rather than external transport. For stirring speeds of 300, 600, and 900 rpm, the film mass transfer coefficients calculated from Eqs. (8)–(12) were 1.03×10^{-2}, 1.64×10^{-2}, and 1.90×10^{-2} cm·s^{-1}, respectively.

Although both the experimental and the calculated curves agree well, the curves at the early stage show a larger discrepancy at lower stirring speed. This may be attributed to the fact that the low stirring speed results in a greater amount of PAC accumulation on the membrane surface.

Effect of Feed (Phenol) Concentration and Flow Rate

Breakthrough profiles for different feed concentrations and varying feed rate are displayed in Figs. 7 and 8, respectively. As would be expected, the breakthrough point is approached more rapidly at a greater flow rate and for a higher concentration of the feed. When the breakthrough curves for the same amount of phenol fed into the cell are compared, the feed flow rate has a more substantial effect on the curve than the feed concentration. This suggests that residence time is an important parameter for the successful design and operation of this system. For both Figs. 7 and 8 the predicted curves agree well with the experimental data. The value of 3.3 × 10^{-8} $cm^2 \cdot s^{-1}$ for surface diffusivity obtained from Fig. 4 data was used.

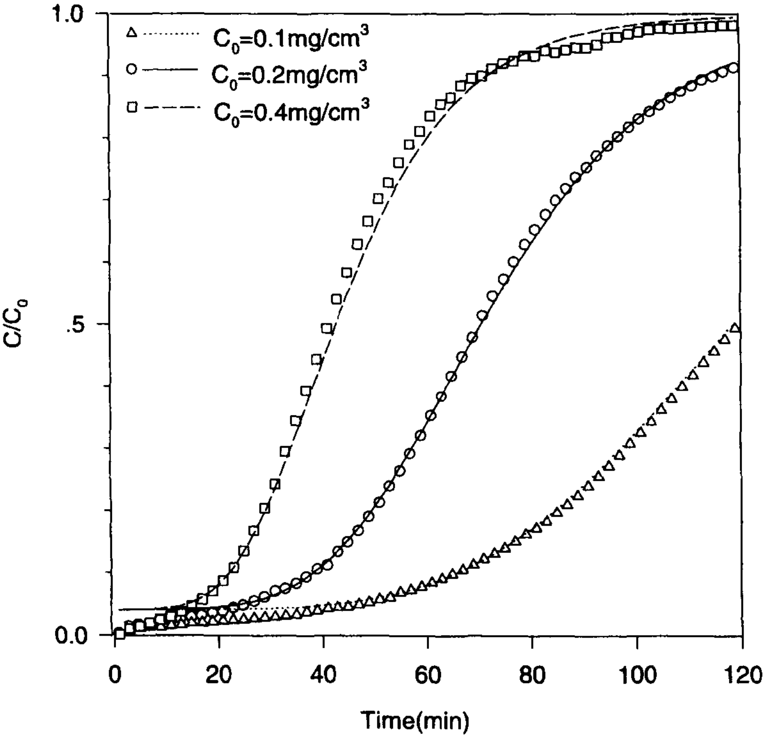

FIG. 7 Breakthrough curves for different feed (phenol) concentrations. The symbols represent experimental data and the lines represent predicted profiles. $V' = 0.19$ cm^3/s, $M_{AC} = 1.2$ g, $V_{holdup} = 70$ cm^3, $N = 600$ rpm.

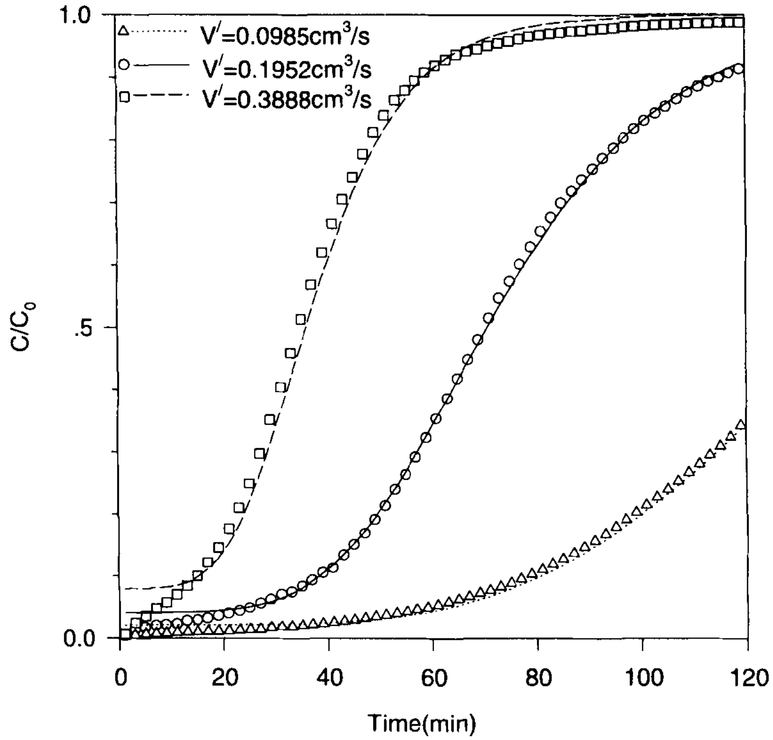

FIG. 8 Breakthrough curves for different flow rates. The symbols represent experimental data and the lines represent predicted profiles. $C_0 = 0.2$ mg/cm³, $M_{AC} = 1.2$ g, $V_{\text{holdup}} = 70$ cm³, $N = 600$ rpm.

CONCLUSIONS

Adsorption of phenol on PAC followed a typical Freundlich isotherm. Intraparticle diffusion appears to be the rate-limiting step in a continuous flow membrane system containing powdered activated carbon (PAC) for phenol removal. The surface diffusion model, which is typically used for the description of packed-bed adsorption with large particles, was employed in a continuous flow membrane system containing powdered activated carbon.

The model agrees well with the experimental breakthrough data obtained for conditions with varying amounts of PAC, holdup volume, stirring speed, feed concentration, and feed flow rate. Surface diffusivity (D_s)

obtained by fitting the model breakthrough curve to that of the experiment was $3.3 \times 10^{-8}\ \mathrm{cm^2 \cdot s^{-1}}$.

There are minor effects of holdup volume and stirring speed on the breakthrough behavior. When the breakthrough curves for the same amount of phenol are compared, the feed flow rate has a more substantial effect on the curve than the feed concentration, suggesting that residence time is an important parameter for the successful design and operation of this system. This agrees with the limiting step being intraparticle diffusion.

ACKNOWLEDGMENTS

The authors gratefully acknowledge funding from the Australian Government for the Centre for Membrane Science and Technology at the University of New South Wales, and from the Korea Science and Engineering Foundation (KOSEF) for a postdoctoral fellowship to support H.W.L.

NOMENCLATURE

A_m	membrane surface area ($\mathrm{cm^2}$)
C	concentration of phenol in bulk liquid ($\mathrm{mg \cdot cm^{-3}}$)
C_e	concentration in liquid phase at equilibrium ($\mathrm{mg \cdot cm^{-3}}$)
C_i	initial concentration ($\mathrm{mg \cdot cm^{-3}}$)
C_s	concentration in liquid outer surface of particle ($\mathrm{mg \cdot cm^{-3}}$)
C_0	inlet concentration ($\mathrm{mg \cdot cm^{-3}}$)
d_I	impeller diameter (cm)
d_p	average particle diameter (cm)
D_m	molecular diffusity ($\mathrm{cm^2 \cdot s^{-1}}$)
D_s	surface diffusivity ($\mathrm{cm^2 \cdot s^{-1}}$)
E_D	energy dissipation rate in slurry per unit mass of particle-free liquid ($\mathrm{erg \cdot cm^3}$)
F	feed concentration ($\mathrm{mg \cdot cm^{-3}}$)
K	Freundlich constant $[(\mathrm{mg \cdot g^{-1}})(\mathrm{mg \cdot cm^{-3}})^{-1/n}]$
k_f	film mass transfer coefficient ($\mathrm{cm \cdot s^{-1}}$)
M_{AC}	mass of activated carbon in suspension (g)
N	stirring speed of impeller (rpm)
N_p	power number (—)
n	Freundlich constant (—)
P	power consumption of the slurry due to agitation ($\mathrm{erg \cdot s^{-1}}$)
ΔP	pressure difference (Pa)
q	solute concentration in solid phase ($\mathrm{mg \cdot g^{-1}}$)

q_e	solid phase concentration in equilibrium with C_c ($mg \cdot g^{-1}$)
q_s	solute concentration at particle surface ($mg \cdot g^{-1}$)
R	particle radius (cm)
R_m	membrane resistance, $\Delta P A_m / \mu V'$ (cm^{-1})
r	radial distance from center of spherical particle (cm)
Re_p	Reynolds number, defined by Eq. (10) or (11) (—)
Sc	Schmidt number, V/D_m (—)
Sh_p	Sherwood number, $d_p k_f / D_m$ (—)
t	time(s)
U	feed flow rate ($cm^3 \cdot s^{-1}$)
V_{holdup}	holdup volume of slurry in stirred cell (cm^3)
V'	permeate rate ($cm^3 \cdot s^{-1}$)
W	mass of particle-free liquid in stirred in stirred cell (g)

Greek Letters

ϵ	volume fraction of liquid (—)
ν	kinematic viscosity ($cm^2 \cdot s^{-1}$)
η	eddy size, defined by Eq. (9) (cm)
ρ_L	density of particle-free liquid ($g \cdot cm^{-3}$)
ρ_P	true density of activated carbon particles ($g \cdot cm^{-3}$)
μ	vicosity ($g \cdot cm^{-1} \cdot s^{-1}$)

REFERENCES

1. H. H. P. Fang and E. S. K. Chian, *Environ. Sci. Technol.*, *10*(4), 364 (1976).
2. G. L. Amy, B. C. Alleman, and C. B. Cluff, *J. Environ. Eng.*, *116*, 200 (1990).
3. R. Rautenbach and S. Klatt, in *Proceedings of 5th International Conference on Pervaporation Processes in the Chemical Industry* (R. Baskish, Ed.), Heidelberg, Germany, March 1991, pp. 392–408.
4. T. Kataoka, T. Nishiki, and S. Kimura, *J. Membr. Sci.*, *41*, 197 (1989).
5. A. M. Urtiaga, M. I. Ortiz, and A. Irabien, *Inst. Chem. Eng. Symp. Ser.*, *119*, 35 (1990).
6. F. F. Zha, A. G. Fane, and C. J. D. Fell, *Sep. Sci. Technol.*, *29*(17), 2317 (1994).
7. O. Eichstadt, Diplomarbeit Thesis, University of New South Wales, 1992.
8. M. Rumeau, F. Persin, V. Sciers, M. Persin, and J. Sarrazin, *J. Membr. Sci.*, *73*, 313 (1992).
9. V. Mavrov, I. Petrova, K. Davarsky, and S. Manolov, *Desalination*, *83*, 289 (1991).
10. Y. I. Dytnersky, K. A. Volcheck, and N. B. Polyanskaya, *Ibid.*, *81*, 273 (1991).
11. R. T. Huang, T. L. Chen, and H. S. Weng, *Sep. Sci. Technol.*, *30*(13), 2731 (1995).
12. W. J. Webber Jr., *Adsorption Theory, Concept and Models, in Adsorption Technology* (F. L. Sleiko, Ed.), Dekker, New York, NY, 1985, pp. 1–65.
13. B. M. van Vliet and W. J. Webber Jr., *J. Water Pollut. Control Fed.*, *53*(11), 1585 (1981).
14. R. T. Huang, T. L. Chen, and H. S. Weng, *Sep. Sci. Technol.*, *29*(15), 2019 (1994).

15. G. S. G. Beveridge and R. S. Schechter, *Optimization: Theory and Practice*, McGraw-Hill, New York, NY, 1970, p. 189.
16. K. J. Kim, V. Chen, and A. G. Fane, *J. Colloid Interface Sci.*, *155*, 347 (1993).
17. H. Freundlich, *Colloid and Capillary Chemistry*, Methuen and Co., London, 1926.
18. W. E. Ranz and W. R. Marshall, *Chem. Eng. Prog.*, *48*, 141 (1952).
19. R. Shinnar and J. M. Church, *Ind. Eng. Chem.*, *52*(3), 253–256 (1960).
20. D. M. Levins and J. R. Glastombury, *Chem. Eng. Sci.*, *27*, 537 (1972).
21. J. H. Rushton and J. Y. Oldshue, *Chem. Eng. Prog.*, *49*(4), 161 (1953).
22. J. H. Rushton and E. W. Costich, and H. J. Everett, *Ibid.*, *46*(8), 395 (1950).
23. C. R. Wilke and P. Chang, *AIChE J.*, *1*, 264 (1955).
24. M. Streat, J. W. Patrick, and M. J. Camporro Perez, *Water Res.*, *29*, 467–472 (1995).
25. J. C. Crittenden and W. J. Weber Jr., *J. Environ. Eng., Div. Am. Soc. Civ. Eng.*, *104*, EE2, 185 (1978a).
26. G. A. Sorial, M. T. Suidan, R. D. Vidic, and S. W. Maloney, *J. Environ. Eng.*, *119*(6), 1044–1058 (1993).

Received by editor March 9, 1996
Revision received December 1996